14th International Symposium on Turbulence and Shear Flow Phenomena (TSFP14)
Heidelberg, Germany, July 28–31, 2026

EXPERIMENTS AND NUMERICAL STUDIES ON TRAVELING WAVY WALL FOR DRAG REDUCTION IN ZERO-PRESSURE-GRADIENT TURBULENT BOUNDARY LAYER

Yasuhiro Yoshida
Faculty of Engineering
Tokyo University of Agriculture and Technology
2-24-16 Nakacho, Koganei, Tokyo, Japan
yoshiday@iis.cc.u-tokyo.ac.jp

(Present affiliation: Institute of Industrial Science
The University of Tokyo
4-6-1 Komaba, Meguro, Tokyo, Japan)

Akira Murata
Faculty of Engineering
Tokyo University of Agriculture and Technology
2-24-16 Nakacho, Koganei,Tokyo, Japan
murata@cc.tuat.ac.jp

Kaoru Iwamoto
Faculty of Engineering
Tokyo University of Agriculture and Technology
2-24-16 Nakacho, Koganei, Tokyo, Japan
iwamotok@cc.tuat.ac.jp

ABSTRACT

Traveling wave wall forcing is a promising approach for turbulent drag reduction, but its streamwise development over a finite control length remains unclear in spatially developing boundary layers. In this study, the streamwise development of turbulence modification over a traveling wavy wall is investigated using experiments and direct numerical simulation (DNS) in a zero-pressure-gradient turbulent boundary layer. In the experiment, a traveling wave is generated by oscillating the upstream edge of a thin flexible rubber sheet, producing wave parameters within ranges known to be effective for turbulence attenuation in fully developed internal flows. Particle image velocimetry (PIV) measurements are conducted at multiple downstream locations over a finite control length of approximately eleven wavelengths. The experimental results indicate a two-stage process of turbulence modification, namely, initial turbulence suppression appears immediately in the near-wall region, and subsequently the turbulence suppression effect gradually spreads toward the outer region of the boundary layer. This streamwise evolution is interpreted within an internal boundary layer framework, in which the thickness of the turbulence-attenuated region grows downstream following a power-law relation. To extend the analysis beyond the experimentally accessible control length, DNS is performed with a streamwise control length of up to approximately 30 wavelengths using parameters comparable to the experiment. The DNS results confirm the upstream experimental trend and extend the analysis toward a quasi-equilibrium state, where turbulence suppression penetrates most of the boundary layer. These results clarify the streamwise development of turbulence suppression induced by traveling wave control and suggest the control length required to approach a quasi-equilibrium state.

INTRODUCTION

Skin-friction drag in wall-bounded turbulent flows is primarily associated with momentum transfer induced by turbulent fluctuations. Reducing such fluctuations leads to a reduction in skin-friction drag, and various flow-control strategies have therefore been proposed to suppress turbulence. Among these strategies, streamwise traveling wave forcing with wall-normal actuation has been identified as an effective approach for reducing turbulent drag (Fukagata *et al.*, 2024). In this method, a sinusoidal wave propagates in the streamwise direction while imposing wall-normal motion, directly interacting with near-wall turbulence. Previous studies have demonstrated that relaminarization or strong turbulence attenuation occurs when the traveling wave parameters fall within specific non-dimensional ranges: amplitudes of $3 \lesssim \eta^+ \lesssim 10$, wavelengths of $200 \lesssim \lambda^+ \lesssim 600$, and wave speeds exceeding the laminar centerline velocity (Nakanishi *et al.*, 2012; Mamori *et al.*, 2014). These parameter ranges have mainly been identified in fully developed internal flows such as turbulent channel and pipe flows.

Although traveling wave control has been extensively studied in fully developed turbulent channel and pipe flows under streamwise periodic boundary conditions, studies of spatially developing flows remain limited. Understanding this streamwise development is important because drag-reduction techniques must be implemented over a finite streamwise length in practical applications. We therefore investigate the streamwise development in a spatially developing turbulent boundary layer. In such flows, the response of turbulence to a sudden change in wall condition is often interpreted using the concept of an internal boundary layer (IBL), which describes how the influence of the wall modification gradually penetrates into the outer region (Hanson & Ganapathisubramani, 2016; Li

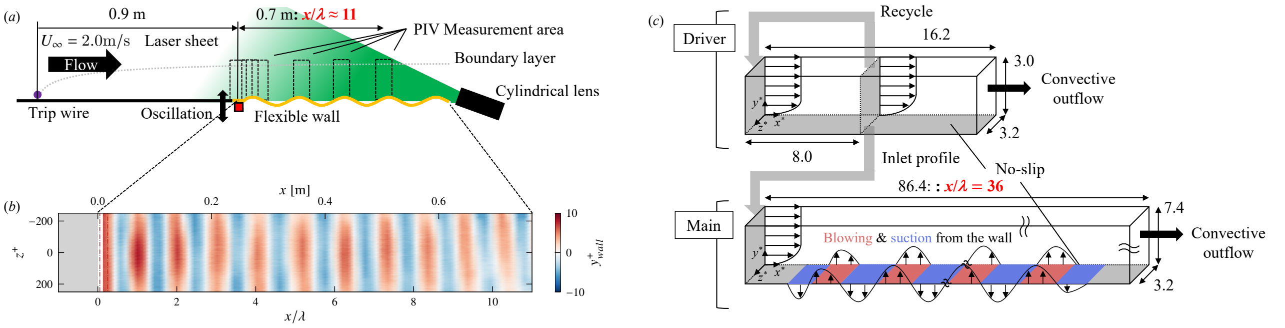

Figure 1. (*a*) Schematic of turbulent boundary wind tunnel of zero-pressure-gradient (side-view). (*b*) Quasi-instantaneous traveling wavy wall deformation obtained by inline laser profile meter (top-view). (*c*) Schematic of computational domain of turbulent boundary layer flow using recycle method (Lund *et al.*, 1998). In (*a*) and (*b*), figures are adopted from Yoshida *et al.* (2026).

et al., 2022). The streamwise growth of the IBL thickness is often described by a power law,

$$\delta_i(x) = ax^b, \tag{1}$$

where a and b are empirical constants.

Recently, Yoshida *et al.* (2025) experimentally demonstrated that a traveling wavy wall generated using a flexible rubber sheet achieves a drag reduction of 9.4% in a zero-pressure-gradient turbulent boundary layer, even when the control region is limited to a finite streamwise length. The traveling wave parameters were chosen to match the effective ranges identified in fully developed flows, and the observed drag reduction was attributed to suppression of turbulent fluctuations. Yoshida *et al.* (2026) further conducted particle image velocimetry (PIV) measurements at multiple streamwise locations over the traveling wavy wall. Their results revealed that turbulence suppression develops through a two-stage process: an initial near-wall attenuation directly induced by the wall motion, followed by a downstream diffusion of reduced fluctuations toward the edge of the boundary layer. This evolution was successfully interpreted within an IBL framework, in which the thickness grows downstream following the power law in Eq. (1). However, the experimentally achievable control length was limited to approximately eleven wavelengths, restricting direct observation of the downstream approach toward a quasi-equilibrium state.

In the present study, we extend these previous experimental findings by combining PIV measurements with direct numerical simulation (DNS) to investigate the streamwise evolution of turbulence modification over substantially longer control lengths. Using traveling wave parameters comparable to those employed in previous experiments, DNS is performed over a streamwise domain extending to approximately 30 wavelengths. By comparing the experimental and numerical results, we examine whether the IBL framework remains applicable as the turbulence suppression progressively extends from the wall toward the edge of the boundary layer and the flow approaches a quasi-equilibrium state.

EXPERIMENTAL AND NUMERICAL SETUP

An experiment was conducted in a zero-pressure-gradient turbulent boundary layer wind tunnel as illustrated in Fig 1*a*. The wind tunnel consists of 0.9 m of flow development section with stationary wall and 0.7 m of control section for traveling wave control with flexible rubber sheet. Two-dimensional PIV measurements in the x–y plane were performed at six streamwise stations in the spanwise center of the wind tunnel. Seeding was operated with silicon oil with a diameter of 1 μm. PIV measurements are performed at x = 1.6 [m] with an area of 80 (streamwise) × 70 (wall-normal) mm^2, which corresponds to 510×440 wall units, by a high-speed CCD camera with a resolution of 1360×1024 pixel^2. We obtained 2590 pairs of images at the recording rate of 15 Hz, which is strictly one-tenth of the frequency of the wall deformation, with a pulse delay of 200 μs to obtain ten different temporal phase information. The streamwise length of the controlled region was approximately 11λ, where λ is the traveling wave wavelength. Experiments were conducted at free stream velocity $U_\infty = 2.0$m/s and resultant Reynolds number based on a momentum thickness in the control section develops from $Re_\theta = 620$ to 880, and the friction Reynolds number develops from $Re_\tau = 260$ to $Re_\tau = 330$. The traveling wave was generated by oscillating the upstream end of the flexible rubber sheet using the piezoelectric actuator (Yoshida *et al.*, 2025). Figure 1*b* is a quasi-instantaneous wave deformation in the x–z plane obtained by a high-speed inline laser profiler (LJ-V7300, KEYENCE Corp.). The wave characteristics, e.g., amplitude $\eta^+ \approx 5$, wavelength $\lambda^+ \approx 440$, and wave speed $c/U_\infty \approx 5$ were confirmed as they are within the effective range proposed previously (Nakanishi *et al.*, 2012; Mamori *et al.*, 2014; Koganezawa *et al.*, 2019).

DNS of a ZPG-TBL with wall-normal blowing and suction to mimic the traveling wave wall forcing was performed to extend the control length and probe farther downstream development. Figure 1*c* shows the schematic of computational domain with streamwise length of about 36λ, corresponding to approximately three times longer than the experimental control section. Governing equations are the incompressible continuity and Navier-Stokes (NS) equations. A developed TBL was introduced at the inflow using a recycling method (Lund *et al.*, 1998). Grid spacings were $(\Delta x^+, \Delta y^+, \Delta z^+) = (8.5, 0.1-50, 4.25)$ representative conditions included $Re_\theta \approx$ 300–800 ($Re_\tau \approx$ 130–340). Traveling wave parameters in the DNS were chosen close to the experiment (e.g. $\eta^+ = 6.2$, $\lambda^+ = 408$, $c/U_\infty = 3.0$).

RESULTS AND DISCUSSION

According to Hussain & Reynolds (1970), instantaneous velocity $\mathbf{u}$ is decomposed as follows:

$$\mathbf{u} = \bar{\mathbf{u}} + \tilde{\mathbf{u}} + \mathbf{u}'', \tag{2}$$

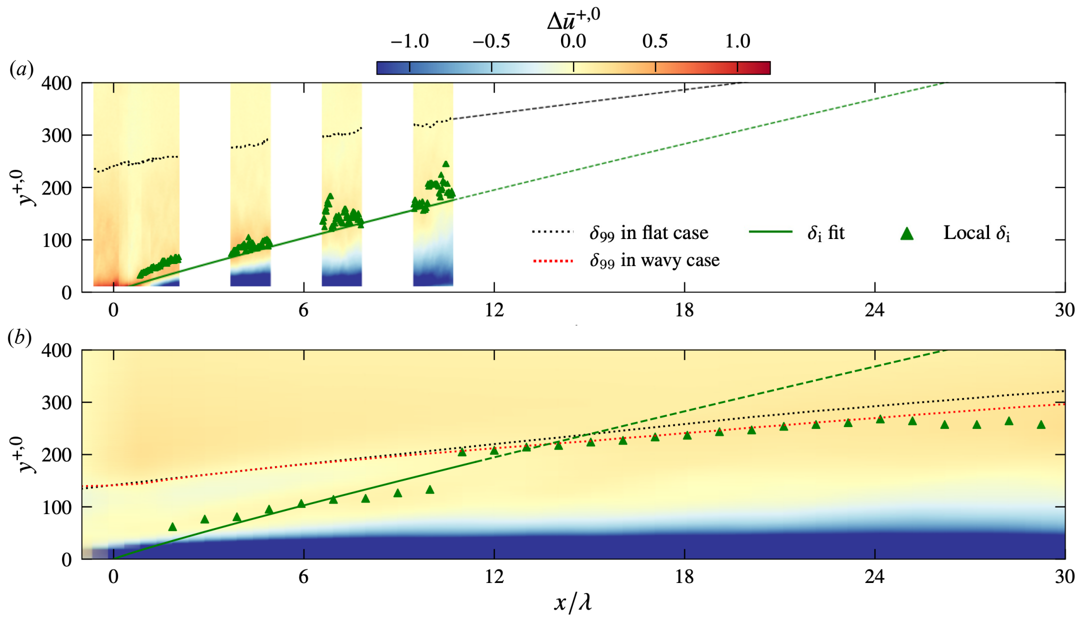

Figure 2. Local change of streamwise random Reynolds shear stress $\Delta\bar{u}$ in (*a*) experiment and (*b*) DNS. Positive value indicate increase due to traveling wave control and vice versa. Experimental data (*a*) and fitting curves are adopted from Yoshida *et al.* (2026).

Table 1. Coefficients a and exponent b for each δ_i in Eq. (1) (Yoshida *et al.*, 2026).

Type of δ_i	a	b
maximum peak of $\Delta\bar{u}$	0.09	0.92
outer peak of $\Delta u''_\mathrm{rms}$	0.1	0.95
inner peak of $\Delta u''_\mathrm{rms}$	0.04	0

where $\bar{\mathbf{u}}$, $\tilde{\mathbf{u}}$, and $\mathbf{u}''$ denotes time-average, periodic velocity fluctuation in the same period of the traveling wave, and random velocity fluctuation, respectively. The fluctuation energy of $\tilde{\mathbf{u}}$ and $\mathbf{u}''$ indicate control input and remained turbulence, respectively, in the boundary layer. When the traveling wave speed is equal to or greater than free stream velocity, i.e., $c \geq U_\infty$, the periodic velocity fluctuation exhibits characteristic streamline patterns in drag-reducing traveling wavy wall (Shen *et al.*, 2003; Koganezawa *et al.*, 2019; Yoshida *et al.*, 2025), namely, streamlines are initiating from the upward motion of the wall and terminate in the downward motion. The flow is attached to the wavy wall with $c \geq U_\infty$, while that is separated from the crest of the wall in wavy wall with $c \lesssim U_\infty$ or steady wall with $c = 0$. Meanwhile, the fluctuation energy of random components exhibits modified turbulent structure since the energy spectrum is similar to typical turbulent structure, for example, streamwise length scale of streamwise velocity fluctuation in wall units is $\mathscr{O}(10^3)$ in the buffer layer (Yoshida *et al.*, 2025). Since the flow pattern of $\tilde{\mathbf{u}}$ considered reducing the fluctuation of $\mathbf{u}''$, periodic and random components are considered direct and secondary effect of the control. Local change in terms in right-hand-side in Eq. (2) due to the traveling wavy wall are then calculated as;

$$\Delta f = f^\mathrm{wavy} - f^\mathrm{flat}, \qquad (3)$$

where Δf denotes local change of given variables f due to the control.

To facilitate the interpretation of Figs. 2 and 3, we introduce an IBL thickness δ_i as the wall-normal location of representative extrema in the local changes induced by the control. For $\Delta\bar{u}$, δ_i is defined as the location of the outer peak, whereas for $\Delta u''_\mathrm{rms}$ it is defined from the outer and inner minima. The downstream evolution of these locations is shown locally in Figs. 2 and 3 and will be summarized in Figs. 4 and 5.

Figure 2 shows the local change of the mean velocity $\Delta\bar{u}$ due to the control. In this figure, the origin of the streamwise coordinate ($x = 0$) is aligned with the starting location of the control, with its length normalized by the wavelength. The wall-normal coordinate is normalized by the u_τ at $x = 0$, indicated by superscript '+,0'. In both the experiment and the DNS, a positive-velocity-change region appears downstream of the control onset and extends progressively toward the outer part of the boundary layer. The wall-normal location of the outer peak, taken here as δ_i, moves upward with increasing x/λ, indicating that the mean-flow modification penetrates farther away from the wall as the flow develops downstream. Although the experimental and numerical conditions are not identical, both results exhibit the same qualitative trend in the upstream region, where the modified layer remains thinner than the boundary layer thickness and grows gradually in the wall-normal direction. For a guide to the eye, we adopt a fitting result of IBL thickness $\delta_\mathrm{i}(x)$ as the wall-normal location of the local peak in $\Delta\bar{u}^+$.

Figure 3 shows the local change in the random streamwise velocity fluctuation, $\Delta u''_\mathrm{rms}$. In both the experiment and the DNS, the fluctuation field is characterized by a near-wall reduction region and an outer reduction region, separated by an intermediate region of increase. The wall-normal position of the inner minimum remains nearly constant with downstream distance, whereas the outer minimum moves progressively away from the wall. As in Fig. 2, the experimental and numerical results show consistent qualitative behavior within the overlap region of the control length.

These observations indicate that the near-wall attenua-

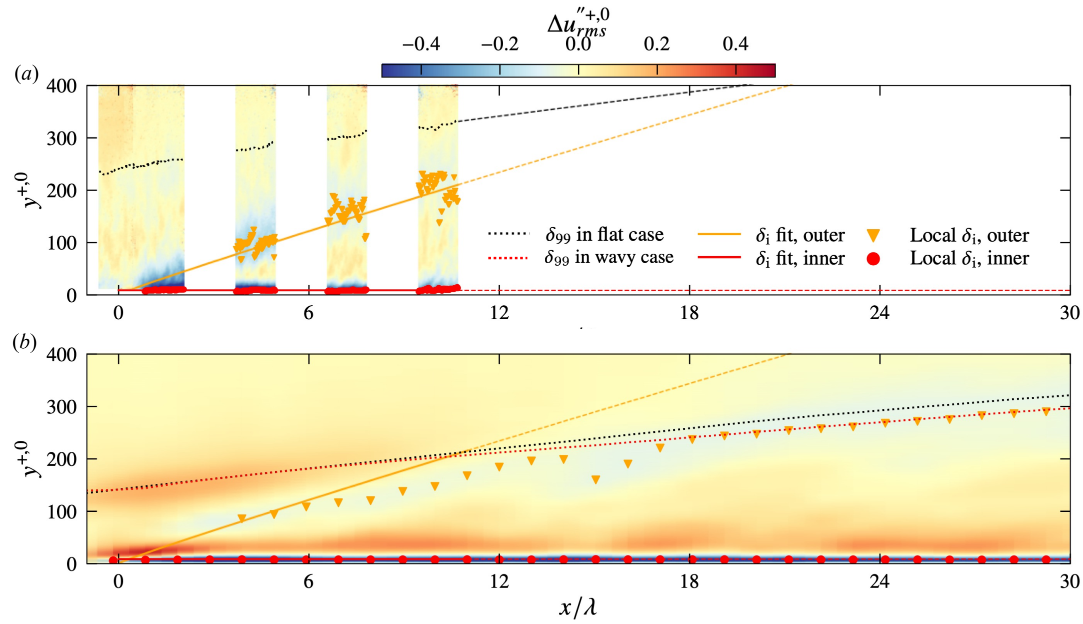

Figure 3. Local change of streamwise random velocity fluctuation $\Delta u''_{\rm rms}$ in (*a*) experiment and (*b*) DNS. Positive value indicate increase due to traveling wave control and vice versa. Experimental data (*a*) and fitting curves are adopted from Yoshida *et al.* (2026).

tion layer is established immediately downstream of the control onset, while the outer-region modification develops more gradually in the downstream direction In the previous studies (Mamori *et al.*, 2014; Yoshida *et al.*, 2025), the direct and the secondary effect are classified using the periodic and the random component in Eq. (1). However, the near-wall direct effect was also indicated in the random component by the present observation of spatial development. The intermittent increase region of $u''_{\rm rms}$ is due to the enhancement of their production $(\mathrm{d}u/\mathrm{d}y)(-\overline{u''v''})$, in the corresponding region (Yoshida *et al.*, 2026).

Figure 4 summarizes the streamwise evolution of the characteristic wall-normal locations identified from $\Delta\bar{u}$ and $\Delta u''_{\rm rms}$, together with the 99% boundary layer thickness. In the upstream region covered by the experiment, the outer peak of $\Delta\bar{u}$ and the outer minimum of $\Delta u''_{\rm rms}$ both exhibit a monotonic downstream growth that is well approximated by a power law. The DNS results follow the extrapolated experimental trend beyond the accessible control length, indicating that the turbulence-modified layer continues to grow farther downstream. In contrast, the inner minimum of $\Delta u''_{\rm rms}$ remains nearly constant in wall-normal position, suggesting that the near-wall attenuation layer is established rapidly and exhibits little downstream growth. As the outer branch approaches the 99% boundary layer thickness, the controlled flow tends toward a quasi-equilibrium state in which the influence of the traveling wave forcing extends over most of the boundary layer.

Figure 5 provides a physical interpretation of the downstream development summarized in Fig. 4 in terms of a two-stage process of turbulence modification. In the first stage, a near-wall attenuation layer is formed immediately downstream of the control onset by the direct action of the traveling wave forcing. This layer remains confined close to the wall and exhibits little streamwise growth in wall-normal extent. In the second stage, the suppression effect gradually spreads toward the outer region of the boundary layer, forming an IBL-like structure whose thickness increases downstream. As the control region extends farther downstream, these two layers progressively merge, and the controlled flow approaches a quasi-equilibrium state in which the influence of the forcing extends over most of the boundary layer.

This interpretation also explains why an appreciable reduction in the boundary layer thickness does not appear immediately downstream of the control onset. In the upstream region, the control effect is primarily confined to the near-wall layer, while the outer part of the boundary layer remains only weakly affected. Only after the outer modified layer has developed sufficiently far downstream does the influence of the control reach the boundary layer edge, leading to a measurable decrease in the 99% boundary layer thickness. This explains why no clear boundary layer thinning is observed within the experimentally accessible control length, whereas a distinct reduction emerges in the DNS with its longer streamwise domain. The delayed onset of boundary layer thinning highlights the importance of sufficiently long control lengths when the objective is to influence not only the near-wall turbulence but also the outer-layer structure of the boundary layer.

It is important to note that the wall-normal coordinate for characterizing this evolution is most appropriately scaled in viscous units. This scaling implies that the streamwise distance required to reach the quasi-equilibrium state is expected to increase with Reynolds number. Such a Reynolds-number dependence could not be inferred from the finite-length experimental data alone in Yoshida *et al.* (2026) and therefore represents a novel insight enabled by the present combination of experiment and DNS. Nevertheless, since the present study is conducted at relatively low Reynolds numbers, the quantitative Reynolds-number dependence of the streamwise development and the approach to quasi-equilibrium should be interpreted with caution.

Despite being defined from different statistical quantities, namely the mean velocity and the random velocity fluctuation, the IBLs identified from the outer-region behavior of $\Delta\bar{u}$ and $\Delta u''_{\rm rms}$ exhibit nearly identical streamwise growth in both the experiment and the DNS. This correspondence suggests that the traveling wave control progressively modulates turbulent motions beyond the immediate near-wall region. Such behav-

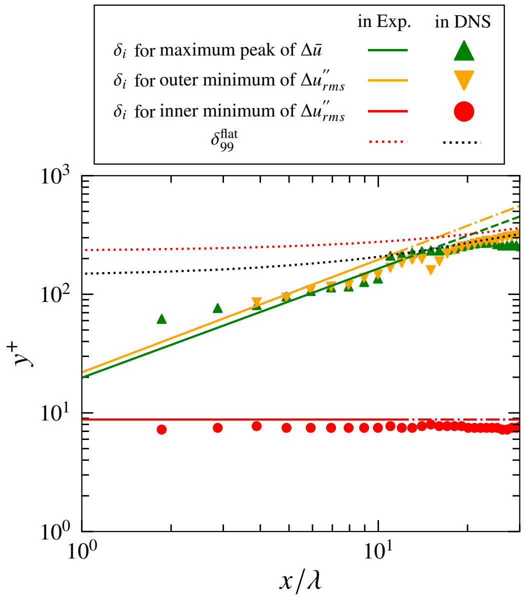

Figure 4. Streamwise evolution of IBL thickness based on $\Delta\bar{u}$ and $\Delta u''_{\mathrm{rms}}$ and 99% boundary layer thickness in Experiment and DNS. Fitting lines from experiments in $x \lesssim 11$ is shown in solid lines and $x \gtrsim 11$ is dot-dashed lines to show the former is the interpolation within previous study (Yoshida *et al.*, 2026), while the latter is extrapolation in the streamwise direction.

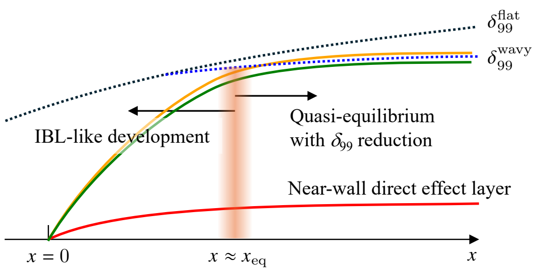

Figure 5. Schematic of the spatial development of the modified TBL over a traveling wavy wall. The control effect propagates from the near-wall direct effect layer to the outer layer, eventually reaching a quasi-equilibrium state characterized by total boundary layer thinning. Line colors indicate type of δ_{i} inheriting those in Fig. 4.

ior may be interpreted in the context of outer-layer turbulence frameworks, including mixing length theory and attached eddy models, although a more definitive assessment would require further analysis at higher Reynolds numbers.

CONCLUSIONS

The streamwise development of turbulence modification in a zero-pressure-gradient turbulent boundary layer (ZPG-TBL) over a traveling wavy wall was investigated using complementary particle image velocimetry (PIV) experiments and direct numerical simulations (DNS). The study provides the following key insights:

Two-stage Modification Process: Turbulence modification progresses through two distinct stages: an immediate attenuation in the near-wall region driven by direct wall forcing, followed by a gradual downstream diffusion of the suppression effect toward the outer boundary layer.

Internal Boundary-Layer Framework: The growth of the modified region is successfully characterized by an internal boundary layer (IBL) thickness $\delta_i(x)$, which follows a power-law growth. This framework shows high consistency across different statistical quantities, including mean velocity and random velocity fluctuations.

Quasi-equilibrium behaviour: While experimental observations were limited by a finite control length of approximately 11λ, the extended DNS domain (36λ) revealed that the controlled flow eventually approaches a quasi-equilibrium state. A measurable reduction in the 99% boundary-layer thickness δ_{99} only emerges once the modification penetrates the entire layer in this downstream state.

ACKNOWLEDGEMENT

This work was supported by JSPS KAKENHI grant numbers JP21H05007, JP21H01245 and JP24KJ1022.

REFERENCES

Fukagata, K., Iwamoto, K. & Hasegawa, Y. 2024 Turbulent drag reduction by streamwise traveling waves of wall-normal forcing. *Annu. Rev. Fluid Mech.* **56**, 69–90.

Hanson, R.E. & Ganapathisubramani, B. 2016 Development of turbulent boundary layers past a step change in wall roughness. *J. Fluid Mech.* **795**, 494–523.

Hussain, A. K. M. F. & Reynolds, W. C. 1970 The mechanics of an organized wave in turbulent shear flow. *J. Fluid. Mech.* **41** (2), 241–258.

Koganezawa, S., Mitsuishi, A., Shimura, T., Iwamoto, K., Mamori, H. & Murata, A. 2019 Pathline analysis of traveling wavy blowing and suction control in turbulent pipe flow for drag reduction. *Int. J. Heat Fluid Flow* **77**, 388–401.

Li, M., De Silva, C.M., Chung, D., Pullin, D.I., Marusic, I. & Hutchins, N. 2022 Modelling the downstream development of a turbulent boundary layer following a step change of roughness. *J. Fluid Mech.* **949** (A7).

Lund, T. S., Wu, X. & Squires, K. D. 1998 Generation of turbulent inflow data for spatially-developing boundary layer simulations. *Journal of Computational Physics* **140** (2), 233–258.

Mamori, H., Iwamoto, K. & Murata, A. 2014 Effect of the parameters of traveling waves created by blowing and suction on the relaminarization phenomena in fully developed turbulent channel flow. *Phys. Fluids* **26** (1), 015101.

Nakanishi, R., Mamori, H. & Fukagata, K. 2012 Relaminarization of turbulent channel flow using traveling wave-like wall deformation. *Int. J. Heat Fluid Flow* **35**, 152–159.

Shen, L., Zhang, X., Yue, D. K. P. & Triantafyllou, M. S. 2003 Turbulent flow over a flexible wall undergoing a streamwise travelling wave motion. *J. Fluid Mech.* **484**, 197–221.

Yoshida, Y., Nimura, T., Mitsuishi, A., Murata, A. & Iwamoto, K. 2025 Drag reduction of turbulent boundary layer flow with traveling wavy wall on flexible rubber sheet. *Phys. Fluids* **37** (7).

Yoshida, Y., Nimura, T., Mitsuishi, A., Murata, A. & Iwamoto, K. 2026 Streamwise evolution of drag-reduced turbulent boundary layer over a travelling wavy wall. *J. Fluid Mech.* **1031**, A44.